Preparation of Bi_2WO_6 Nanoparticles with Improved Photocatalytic Properties by Adding Triblock Copolymer P123

Su-Hua CHEN[1,a], Hong-Mei WAN[1,b], Guo-Ping WU[2,b,*]

[1] School of Environmental and Chemical Engineering, Nanchang Hangkong University, Nanchang 330063, China

[2] College of Food Science and Engineering, Jiangxi Agricultural University, Nanchang 330045, China,

[a]trensuhua@163.com, [b] 462945731@qq.com, [c]* jdwgp@163.com

*Corresponding author

Keywords: Photocatalytic, Bi_2WO_6, Pluronic P123, Visible Light.

Abstract. Nanocrystalline bismuth tungstat with good visible light response has been synthesized using Pluronic P123 triblock copolymer as surfactant. The prepared samples were characterized by X-ray diffraction, UV-visible spectroscopy, scanning electron microscopy, and BET surface area analysis. The activity of the material in photocatalytic decoloration of aqueous rhodamine B (RhB) solution under visible light was evaluated. The results showed that the presence of P123 could improve the crystallization of Bi_2WO_6 species and greatly enlarge their specific surface area. The copolymer concentration has a great impact on the bismuth tungstat morphology. The photocatalytic efficiency of the as-prepared Bi_2WO_6 with P123 adjusted is higher than that of pure Bi_2WO_6.

Introduction

In the past decade, photocatalysts has been attracted great attention for removing organic pollutants in environment and producing clean energy such as H_2 from water. But photocatalytic decomposition of water into H_2 or removal of pollutants has not been applied widely in practice because it is unable to utilize sunlight efficiently. Therefore, the research on the photocatalysts under visible light has been one of the most important issues. Semiconductors that are based on Aurivillius oxides have properties suitable for photocatalytic applications. Bismuth tungstate (Bi_2WO_6), one of the simplest Aurivillius phase oxides, has been used as a new photocatalyst that works under visible light irradiation [1]. These researches found that the catalytic properties of the bismuth tungstate deeply depent on their structures, morphologies and components [2-4].

The structures of nanomaterials, such as particle size, shape and crystallinity, are the key factors that determine the evolution of physical properties in functional nanomaterials. Therefore, the control synthesis of inorganic nanomaterials with different morphologies has been focused recently, for example, the preparation of nanotube, nanowire, nanorod and hollow spheres [5-8]. Many works reported the preparation of Bi_2WO_6 with micro/nano structures including nanoplates, nanoparticles and thin films, and explained their growth mechanisms [2-4]. By using hydrothermal method, Shang et al prepared heterogeneous Bi_2WO_6/TiO_2 nanowire with three dimension structure, which could efficiently degrade ethyl alcohol and Rhodamine B [9]. They ascribed this efficiency to its particle size, specific surface area and hierarchical structure. The microwave synthesis approach was also applied to the preparation of flowerlike Bi_2WO_6 which had good visible light driven catalytic properties [10]. However, more approaches are still discovered to improve the catatlytic activities and morphologies of Bi_2WO_6.

To our knowledge, the addition of P123 can act as both a reducing agent and colloidal stabilizer in the synthesis of nanomaterials that exhibit various sizes and shapes. Thus, in this work, triblock copolymer P123 was applied to prepare Bi_2WO_6 and the transformation of morphology and catalytic property of this resultant Bi_2WO_6 were investigated.

Experimental

Materials

The Pluronic P123 was purchased from Sigma-Aldrich Company. Bismuth nitrate, sodium tungstate, concentrated nitric acid, glacial acetic acid, absolute ethyl alcohol and rhodamine B were commercial product from Shanghai Chemical Reagent Co. Ltd., China. All reagents in this work were of analytical grade and used without further purification as received. Ultrapure water was used throughout the experimental process.

Sample Preparation

For the synthesis of Bi_2WO_6 nanoparticles, firstly the desired amount of triblock copolymer P123 was dissolved in 36.0 ml water at 60 ^{0}C and under vigorous stirring and then Na_2WO_4 $2H_2O$ (0.3258 g) was added to obtain the mixture of P123 and sodium tungstate.1.2127 g of $Bi(NO_3)_3$ $5H_2O$ was dissolved in 3.0 ml of glacial acetic acid. The obtained solution was subsequently added to the mixture of P123 and sodium tungstate and stirred for further 60 min at 60 ^{0}C. The final concentration of P123 in this reaction mixture solution was 10 g/L, 20 g/L, 30 g/L and 40 g/L respectively. It was poured into a stainless steel autoclave with a Teflon liner of 50 mL capacity and maintained at 160 ^{0}C for 24 h. After the autoclave had cooled to room temperature, the products were washed with ultrapure water and absolute ethanol in turn for three times, and later separated centrifugally. The wet gels were dried at 60 ^{0}C for 8 h and then pyrolyzed at 550 ^{0}C for 6 h under a N_2 (99.999%) atmosphere at a ramping rate of 2 ^{0}C/min. As control experiments, Bi_2WO_6 nanoparticles were also synthesized without P123 by a similar procedure.

Characterization

The morphology and size of the resulting Bi_2WO_6 nanoparticles were examined on a JEOL JSM-7401F scanning electron microscopy (SEM) at an accelerating voltage of 20 kV. Powder X-ray diffraction (XRD) was performed on a Bruker D8 Advance X-ray diffractometer using Cu Kα radiation (λ=0.15418 nm) at a scanning rate of 8°/min in the 2θ ranging from 10° to 70°. UV-vis diffuse reflectance spectra of the as-prepared samples were obtained on an UV-vis spectrophotometer (Hitachi U-3900H), using $BaSO_4$ as the reference. N_2 adsorption data were measured using a NOVA 2000e (Quantachrome) instrument at −196 °C after degassing the samples for 10 h under vacuum at 200 ℃, and the specific surface area was calculated by the Brunauer- Emmett-Teller (BET) equation.

Photocatalytic Activity

The photocatalytic procedure of RhB was described as follows. Firstly, a solution containing 1×10^{-5} mol/L RhB and 0.1 g of photocatalyst was prepared and magnetically stirred in the darkness for 60 min. Subsequently, the prepared suspension was kept under UV light irradiation of a 30 W low-pressure mercury lamp. All the experiments were carried out at room temperature. At 20 min intervals, a 4 mL solution was sampled and centrifuged to remove the photocatalyst particles. Then the filtrates were analyzed by recording variations of the absorption band maximum (553 nm) in the UV-vis spectra of RhB by using a Hitachi U-3900H spectrophotometer.

Result and Discussion

Characterization of Bi_2WO_6/P123 Nanoparticles

The XRD patterns of the obtained samples are shown in Fig. 1. Comparing XRD pattern of synthesized particles with the standard diffraction specturum (JCPDS Card NO. 79-2381), the synthesized products are crystalline Bi_2WO_6. In addition, no characteristic peaks of other impurities were observed, which indicated that the products had high purities. The sharpness of the main diffraction peaks clearly shows that they are highly crystalline and the crystallines grew well. However, the intensities of the peaks decreased when the concentration of P123 increased. Sherrer's formula was applied to calculate the average crystallite sizes, which are presented in Table 1. As it can be seen, with increasing the concentration of P123 the crystallite size decreased, especially when

the concentration of P123 increased from 30 g/L to 40g/L, the particle size decreased by nearly 50% from 20.64 nm to 11.35 nm. The XRD patterns of the sample prepared without addition of P123 showed higher intensities for the peaks corresponding with standard Bi_2WO_6 indicating the larger crystallite sizes (Table 1).

Table 1 Textural properties of the materials

Sample	Crystallite size (nm)	SBET (m2g-1)
Bi2WO6	41.28	1.569
10g/L P123/Bi2WO6	41.26	10.35
20g/L P123/Bi2WO6	45.43	10.399
30g/L P123/Bi2WO6	45.4	9.193
40g/L P123/Bi2WO6	113.5	10.349

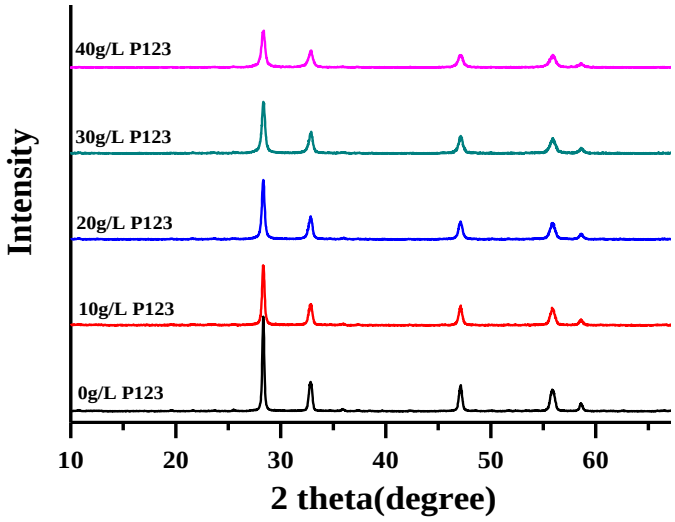

Fig. 1 XRD patterns of the samples synthesized with different amounts of P123 adjusted

The effect of Pluronic P123 block copolymer on the morphology of the Bi_2WO_6 was studied and the results are presented in Fig. 2. It is seen that the presence and the concentration of P123 has a prominent effect on the morphology of the as-synthesized samples. The sample prepared in the absence of P123 exhibited a regular particle morphology consisting of flower-like three-dimensional microspheres with a diameter of about 4 to 5 μm, as shown in Fig. 2(a) and (b). When the P123 concentration was 10 g/L, only some particles are spherical flower-like, while most are flocculent crystals (see Figure 2(c)). With increasing P123 concentration, most particles with a diameter of about 2 to 3 μm display a spherical flower-like shape with some tiny flocculent crystals around the edge as can be seen from Figure 2(d) and (e). However, sample prepared with a P123 concentration of 50 g/L consists of flower-like structures being of spherical outline similar to and of smaller diameter (3 μm) than sample prepared without P123 (see Figure 2(f)). These results indicate that P123 indeed played a role in determining the particle morphology by directing the growth of inorganic Bi_2WO_6 species along a specific crystallographic direction. It may be inferred from the above results that only when the concentration of P123 is below 40 g/L could such a role of P123 be operative under our experimental conditions.

A number of sphere-like microparticles with a diameter of about 4 μm are clearly observed (Figure 2a, c), coexisting with a mass of tiny nanoplates with a rather short edge which we believe are evolved from the original material sources (Figure 2b, d).From Figure 2c it is evident that some MC around Bi_2WO_6 particles，that is a weak van der Waals interaction between them. Clearly, some flower-like Bi_2WO_6 microparticles are obtained (Figure 2d), this structure is the self-assembled spherical

structure from as-formed nanosheets, maybe it can improve this process with the MC. A lot of floc-like MC appear in Figure 2e,f ,and some of the MC samples show rod-like morphology (Figure2 f),showing most of the MC assembled but a few of the MC still retained the original morphology and structure of the silica template.

The width of the fibers increased with the salt concentration. For sample A-5, the fibers are much larger with a typical width of about 1 μm. It thus can be concluded that, simply by changing the salt concentration, the width of the fibers can be tuned from tens of nanometers to 1 μm. Such an effect of the salt concentration on the product morphology may be related to the ion strength of the synthesis system. A higher salt concentration, and thus a higher solution ion strength, leads to the compression of the electrical double layer of the charged primary particles, which results in their rapid coagulation to large particles. Otherwise, the charged primary nanoparticles tend to remain stable in the solution, which gives birth to thinner fibers.

This is understood as such low water content leads P123 and aluminum species to form separate phases during the hydrothermal treatment. With increasing water content, samples H-2 and H-3 showed a regular fibrous morphology. Further increasing the water concentration to a H_2O:Al molar ratio of 280 produced sample H-4 with an irregular morphology. Interestingly, the H-5 sample prepared with a H_2O:Al molar ratio of 330 is made up of bundles of short flakes, which are about 1−2 μm long. Some flakes are even packed into a flowerlike shape (see Figure S4f). A simple explanation of the water effect is that the water concentration determines the aluminum salt concentration, which in turn determines the morphology of the product by influencing the solution ion strength.

The results showed that when low concentrations of P123, the morphology of Bi_2WO_6, has been greatly affected, Bi_2WO_6 whose nanoparticles small particles self-assembly process is not smooth, so some of the nanostructure synthesis floc. When the concentration of P123 is large enough, the effect is not great to Bi_2WO_6, and it can self-assemble into spherical flower-like structure, but no previous large size, indicating that a large concentration of P123, it can only limit size of Bi_2WO_6 , but not affect its shape. The mechanism needs to be deeper research.

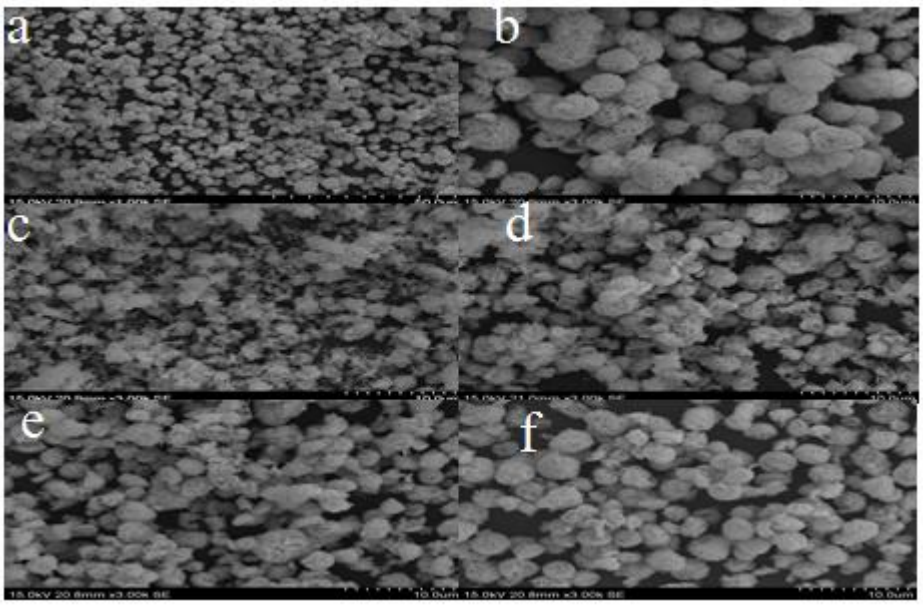

Fig. 2 SEM images of the Bi2WO6 nanocages sample:(a and b) absence of P123, (c)10%P123, (d)20%P123, (e) 30%P123, (f) 40%P123

Optical absorption of various P123/Bi_2WO_6 samples was measured by UV-visible diffuse reflectance spectrum, and the results are shown in Fig. 3. According to the spectra, the as-prepared Bi_2WO_6 samples present the photoadsorption properties from UV light region to visible light, indicating that all of Bi_2WO_6 samples have potential photocatalytic activity under visible light irradiation. The steep shape of the spectrum indicates that the visible light absorption is not due to the

transition from the impurity level but due to the band-gap transition,which is consistent with previous studies[11,12,13]. However, P123 application to the Bi_2WO_6 resulted in an overall no observable adverse effect on its absorption band, because the triblock copolymer P123 act as an non-ionic surfactant that can not be ionized in aqueous solution, thus the triblock copolymer P123 had few effect on the growth of the crystal.

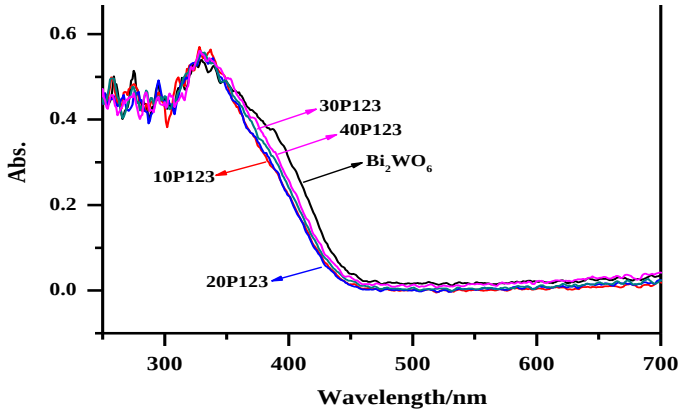

Fig. 3 The UV-vis diffuse reflectance spectrum of the Bi2WO6 nanocages sample

Action Mechanism of P123

The properties of crystal material depend on particle size, impurities in the crystal or the evolution of crystal structure. The crystal of nucleation, growth, copolymerization related to the reaction conditions in the process of crystallization, As we know, P123 commonly used in drug synthesis, biomedical materials, a template synthesis of mesoporous materials and nano particles as scattered stabilizer.

Although the exact role in crystal growth by P123 cannot be fully explained, the mechanism in the nucleation stage of Bi_2WO_6 to prevent crystal nucleus gathered in excess. The WO_4^{2-} surrounded by P123 and form a protected WO_4^{2-}-P123 unit in the reaction solution. When mixed reaction solution, the Bi^{6+} may replace the P123 molecules in WO_4^{2-}-P123 unit and eventually obtain Bi_2WO_6 nanoparticles. The P123 molecules adsorbed in the surface of Bi_2WO_6 to prevent the nucleation rate in the later growth stage. Therefore, some different structure Bi_2WO_6 nanoparticles we have obtained. Such as, the flocculent-Bi_2WO_6 nanoparticles we have get in 10 g/L p123 solution. With the p123 concentration increased, 3D-flower-Bi_2WO_6 nanoparticles we have obtained. That means the growth rate with each crystal face become balance, because of P123 can act as stabilizer in the synthesis of nanomaterials. In the concentration of P123 at 40 g/L reaction conditions, we synthesized microspheres- Bi_2WO_6 nanoparticles, this suggests that the morphology of material is the result of the interaction between crystal growth with the P123 molecular.

Conclusion

In this study, highly crystalline silver microscale nanos-tructures with well-defined shapes of dendrites have beensynthesized via electrodeposition by using P123 as the soft template. It has been found that the concentrations of AgNO3and P123 play significant roles in the growth of the silver dendrites. The results suggest that electrodeposition could be a versatile way to create high surface area electrodes for various applications such as in the fields of batteries and catalysis. This method may be extended to prepare novel nanostructures of other noble metals.

Acknowledgement

The work was financially supported by the Science and Technology Research Foundation of the Provincial Education Department of Jiangxi (GJJ08201), the Natural Scientific Foundation of Jiangxi

Province (CA200802042) and the Innovation Foundation for Graduates of Jiangxi Province (YC10A113).

References

[1] J. Tang, Z. Zou, J. Ye, Photocatalytic decomposition of organic contaminants by Bi2WO6 under visible light irradiation, Catal. Lett. 92 (2004) 53–56.

[2] J. Li, X. Zhang, Z. Ai, et al, Efficient visible light degradation of rhodamine B by a photo-electrochemical process based on a Bi_2WO_6 nanoplate film electrode. J. Phys. Chem. C 111 (2007) 6832-6836.

[3] M. Shang, W. Wang, and H. Xu, New Bi_2WO_6 nanocages with high visible-light-driven photocatalytic activities prepared in refluxing EG. Crystal Growth & Design 9 (2009) 991-996.

[4] L. Zhang, Y. Wang, H. Cheng, et al, Synthesis of porous Bi_2WO_6 thin films as efficient visible-light-active photocatalysts. Adv. Mater. 21 (2009) 1286-1290.

[5] C. Burda, X. B. Chen, R. Narayanan, et al, Chemistry and properties of nanocrystals of different shapes, Chemical Reviews105 (2005)1025-1102.

[6] R. Ostermann, D. Li, Y. Yin, et al, V2O5 nanorods on TiO2 nanofibers: A new class of hierarchical nanostructures enabled by electrospinning and calcination, Nano Lett. 6 (2006)1297-1302.

[7] R. Shi, Y. Wang, D. Li, et al., Synthesis of ZnWO4 nanorods with [100] orientation and enhanced photocatalytic properties, Applied Catalysis B: Environmental 100 (2010) 173-178.

[8] X. Dai, Y. Luo, W. Zhang, et al., Facile hydrothermal synthesis and photocatalytic activity of bismuth tungstate hierarchical hollow spheres with an ultrahigh surface area, Dalton Trans. 39 (2010) 3426-3432.

[9] M. Shang, W. Wang, L. Zhang, et al., 3D Bi2WO6/TiO2 hierarchical heterostructure: controllable synthesis and enhanced visible photocatalytic degradation performances, J. Phys. Chem. C 113 (2009) 14727-14731.

[10] X. Cao, L. Zhang, X. Chen, et al., Microwave-assisted solution-phase preparation of flower-like Bi2WO6 and its visible-light-driven photocatalytic properties. J. Phys. Chem. C 114 (2010) 1001-1014.

[11] L. Zhang, W. Wang, Z. Chen, et al. Fabrication of flower-like Bi2WO6 superstructures as high performance visible-light driven photocatalysts [J]. J. Mater. Chem. 2007,17:2526–2532.

[12]M. Shang, Wenzhong Wang, and Haolan Xu. New Bi2WO6 nanocages with high visible-light-driven photocatalytic activities prepared in refluxing EG [J]. Crystal Growth & Design,2008, 9(2): 991-996.

[13] A. Kudo, I. Tsuji, H. Kato. AgInZn7S9 solid solution photocatalyst for H2 evolution from aqueous solutions under visible light irradiation [J]. Chem. Commun. 2002,17:1958–1959.